Falco UAV Low Reynolds Airfoil Design and Testing at Galileo Avionica

Dr.Ing. Luca Cistriani
UAV Design Engineer
Galileo Avionica Simulators and UAV Business Unit
Via Mario Stoppani, 21
34077, Ronchi Dei Legionari (Gorizia)
ITALY

luca.cistriani@galileoavionica.it

ABSTRACT

UAV operations are examined from a performance and logistic flexibility point of view in order to set up requirements to be input for the multiobjective optimization of a two component simple rotation flap slotted airfoil with high thickness to chord ratio. The airfoil selected among a wide range of geometries optimizing the two design points has been investigated using CFD for stability at low Reynolds numbers and sensitivity to parameters like free stream turbulence and in-flight icing. Wind tunnel tests have been performed for the two dimensional wing section and for a complete UAV aircraft configuration in order to confirm theoretical previsions. Finally, flight tests of the prototype aircraft have been executed with results in good agreement with the previous design and test work.

NOMENCLATURE

A/C	Aircraft
ALSWT	Alenia Low Speed Wind Tunnel
A/P	Autopilot
AR	Aspect Ratio
C_D	Drag Coefficient
CFD	Computational Fluid Dynamics
CMIC	Continuous Maximum Icing Conditions
C.I.R.A.	Centro Italiano Ricerche Aerospaziali (Italian Aerospace Research Center)
C_L	Lift Coefficient
EAS	Equivalent Air Speed
EASA	European Aviation Safety Agency
G.A.	Galileo Avionica
GA-ASI	General Atomics – Aeronautical Systems Inc.

Cistriani, L. (2007) Falco UAV Low Reynolds Airfoil Design and Testing at Galileo Avionica. In *UAV Design Processes / Design Criteria for Structures* (pp. 3.3-1 – 3.3-24). Meeting Proceedings RTO-MP-AVT-145, Paper 3.3. Neuilly-sur-Seine, France: RTO. Available from: http://www.rto.nato.int/abstracts.asp.

Report Documentation Page

Form Approved
OMB No. 0704-0188

1. REPORT DATE	2. REPORT TYPE	3. DATES COVERED
01 NOV 2007	**N/A**	**-**

4. TITLE AND SUBTITLE	5a. CONTRACT NUMBER
Falco UAV Low Reynolds Airfoil Design and Testing at Galileo Avionica	5b. GRANT NUMBER
	5c. PROGRAM ELEMENT NUMBER
6. AUTHOR(S)	5d. PROJECT NUMBER
	5e. TASK NUMBER
	5f. WORK UNIT NUMBER
7. PERFORMING ORGANIZATION NAME(S) AND ADDRESS(ES) **Dr.Ing. Luca Cistriani UAV Design Engineer Galileo Avionica Simulators and UAV Business Unit Via Mario Stoppani, 21 34077, Ronchi Dei Legionari (Gorizia) ITALY**	8. PERFORMING ORGANIZATION REPORT NUMBER
9. SPONSORING/MONITORING AGENCY NAME(S) AND ADDRESS(ES)	10. SPONSOR/MONITOR'S ACRONYM(S)
	11. SPONSOR/MONITOR'S REPORT NUMBER(S)

12. DISTRIBUTION/AVAILABILITY STATEMENT
Approved for public release, distribution unlimited

13. SUPPLEMENTARY NOTES
See also ADM202420., The original document contains color images.

14. ABSTRACT

15. SUBJECT TERMS

16. SECURITY CLASSIFICATION OF:			17. LIMITATION OF ABSTRACT	18. NUMBER OF PAGES	19a. NAME OF RESPONSIBLE PERSON
a. REPORT	b. ABSTRACT	c. THIS PAGE			
unclassified	**unclassified**	**unclassified**	**UU**	**24**	

GCS	Ground Control Station
H24	24 Hours
IAI	Israeli Aircraft Industries
IMIC	Intermittent Maximum Icing Conditions
IR	Infra Red
KCAS	Knots Calibrated Air Speed
L/D	Lift to Drag Ratio
LOS	Line of Sight
LWC	Liquid Water Content
M	Mach Number
MVD	Mean Volume Diameter
OAT	Outside Air Temperature
PISQ	Poligono Interforze del Salto di Quirra
Re	Reynolds Number
STOL	Short Take Off and Landing
TAS	True Air Speed
UAV	Unmanned Aerial Vehicle
U	Velocity Component ad the Edge of Boundary Layer
X	Distance Along the Wall
θ	Boundary Layer Displacement Thickness
ν	Coefficient of Kinematic Viscosity

1.0 INTRODUCTION

1.1 General Concepts

Great interest has been raised recently in both military and civil UAV applications including visible, IR and multi-spectral reconnaissance, border patrol and monitoring, fisheries and wildlife refuge management, atmospheric sampling for validating weather forecast numerical models, chemical and biological agent detection, law enforcement, disaster assistance and monitoring and telecommunications relay.

Despite the multiplicity of missions it is possible however to select a number of major operational requirements. All the above-mentioned applications share the requirement for medium or long endurance, all weather capability, and H24 availability, which in turn involves logistic flexibility. Logistic flexibility means rapid deployment (including STOL characteristics and/or the capability to operate from unprepared surfaces or naval vessels), rapid turn around cycling and fast reconditioning of the air-vehicle.

The major operational requirements are:

- Medium / long endurance
- All weather
- Logistic flexibility

1.2 Performance Requirements for the FALCO UAV

The FALCO UAV constitutes the flying segment of an aerial surveillance system able to perform a wide range of missions for both civil and military applications. The overall maximum take off weight of the UAV is less than 500 kg (1100 lbs) in its heaviest configuration.

The following performance are required:

- Stall speed (EAS) $\leq$ 30 m/s (58 kts)
- Initial rate of climb $\geq$ 6.5 m/s (21 ft/s)
- Maximum ceiling 6000 m (20000 ft)
- Cruise speed $\approx$ 45 m/s (87 kts)
- Endurance according to specific mission requirements
- Line of sight range > 150 km (81 nm)

Stall speed requirements are mainly related to take-off and landing performance but with the “Equivalent Energy” criteria of the EASA classification of UAVs, stall speed could also be directly related to the applicable airworthiness criteria for the civilian type certification of the air vehicle (ref. [1]).

Initial rate of climb is mainly due to the maximum ceiling requirement, which in turn is dominated by the need for silent, safe flying in military operations (especially above hostile territory) and to safety related issues when over flying a populated territory in civilian missions (mainly engine-off gliding range for single engine UAVs). The capability to fly at altitude is also indirectly related to the maximum range requirement since earth curvature influences LOS distance; as an example: on a flat ground, an unmanned aircraft flying at 200 km (108 nm) from its GCS should be able to keep an altitude of at least 3000 m (10000 ft) above the controlling station to keep LOS.

Cruise speed is of interest when it comes to operational requirements involving transfer timings (e.g. time to reach a patrol area) or over flown area per time period (e.g. square km per flight hour); it should be noted however that propeller driven, piston engine, lightweight UAVs optimized for long endurance flight at high altitudes usually have a quite narrow flight envelope in terms of speed. Consequently, the cruise speed requirement of roughly 80-90 kts TAS is actually straightforward with other requirements (the above mentioned stall speed and ceiling requirements).

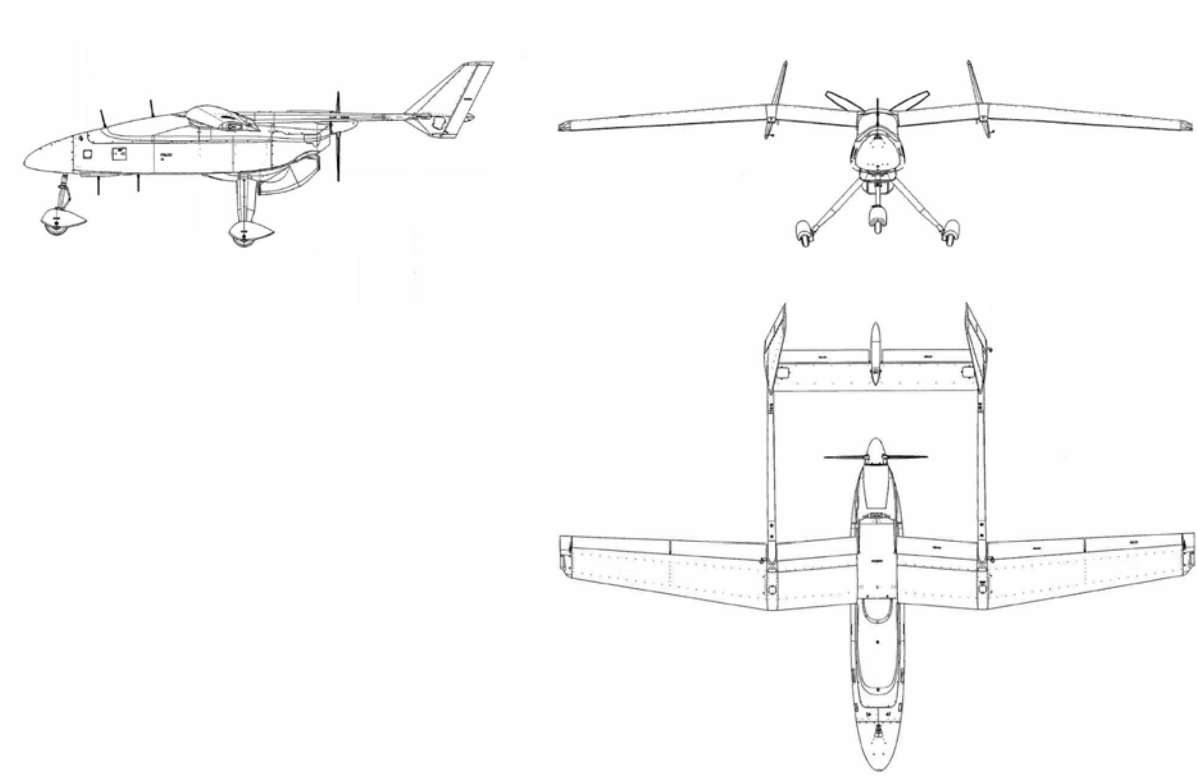

Figure 1: FALCO UAV three views drawing

2.0 REQUIREMENTS FOR WING SECTION DESIGN

Attempting to design a wing section for the family of UAVs described above, the requirements of major concern are the following:

- Medium to long endurance means high L/D ratios for the entire aircraft.
- A high ceiling necessitates a high ceiling parameter: M2CLmax.
- A high initial rate of climb means high values of the parameter CL3/2/CD.
- All weather capability means high wing loadings in order to deal with turbulence and tolerance to adverse atmospheric effects like in-flight rain impingement or ice accretion.
- STOL performances require high CLmax in take-off configuration.

Additional features, either directly linked to specific aerodynamic parameters or indirectly through geometric shape requirements are the following:

- High specific structural resistance is desired in order to keep as low as possible the structural weight allowing for greater payload and/or fuel weight.
- Redundant control surfaces design.
- Small sensitivity to surface imperfections or dirt in order to facilitate logistic flexibility (i.e. operations from unprepared surfaces, small damages deriving from inaccurate handling etc.).
- High thickness to provide volume for fuel inside the wing structure.

To establish the initial design philosophy, it can be observed that historically in the UAV world even quite different aircraft designs have about the same Mean Aerodynamic Chord, that is usually about two feets

(0.6 m) for UAVs ranging from 230 kg of the METEOR Mirach 26 to more than 1.000 kg of the GA-ASI Predator and the IAI Heron. Wing designs are mainly differentiated by their aspect ratio and some early UAV designs have been "revitalized" by adding some meters of wingspan during their career.

UAVs usually have quite high wing loadings (about 100 kg/m^2) if compared to general aviation aircraft of the same size and weight, but in order to maximize the ceiling and power parameters a reduction in the induced drag term of the wing (by maximizing its aspect ratio) is usually preferable to have low loaded, low aspect ratio wings, since airfoil drag cannot be reduced below a certain limit, especially when low Reynolds number are involved. Consequently it could be expected that satisfying performance figures can be realized by designing a wing of relatively high AR (> 10) with a highly loaded airfoil; the overall drag reduction is obtained, despite airfoil drag, by minimizing the actual wing surface with smaller span and chord. The design goal then is to minimize drag as far as practicable at fixed (high) lift coefficient values.

A quite similar design philosophy applied to general aviation turbulent airfoils is discussed by Prof. R. Eppler about the design of the GA(W)-1 airfoil in ref. [2].

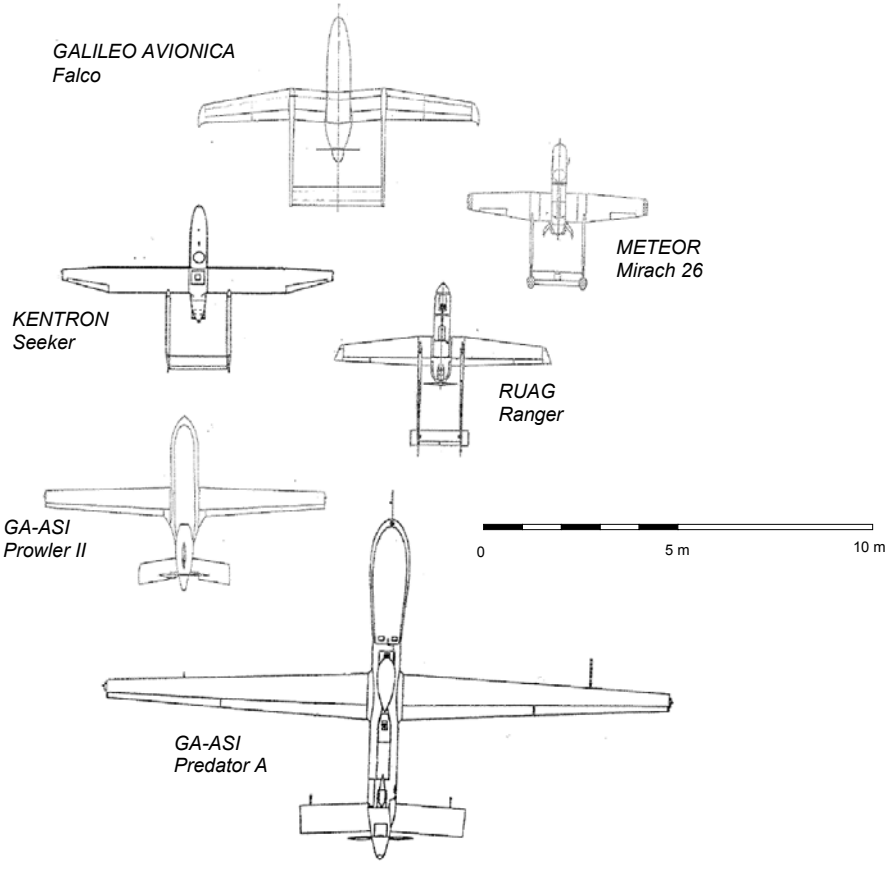

Figure 2: Comparison of different UAV dimensions

Table 1: Typical UAV wing design features (estimated geometrical characteristics)

Air Vehicle	*T/O weight [kg]*	*Wing surf. [m^2]*	*Wing span [m]*	*AR*	*M.A.C. [m]*
Meteor Mirach 26	230	2.94	4.50	6.89	0.669
Kentron Seeker	240	4.24	7.00	11.50	0.628
RUAG Ranger	250	3.41	5.47	8.78	0.648
GA-ASI Prowler II	350	4.46	7.31	11.98	0.600
GA-ASI Predator A	1021	11.09	14.85	19.90	0.800
Galileo Avionica Falco	**430**	**4.53**	**7.20**	**11.44**	**0.664**

3.0 DESIGN AND TESTING CARRIED ON AT GALILEO AVIONICA

3.1 Initial Shape

The first step in the airfoil design carried on at Galileo Avionica for the Falco UAV was the selection of a suitable initial geometry to start a multi-point optimization. The basic starting idea, to obtain high design lift coefficients, was to set up a 2 component airfoil as used in many Ultra-Light STOL applications (perhaps like the well known Fiesler Storch) with a 30% chord ratio simple rotation flap to be used both as an high-lift and roll control device. A 20% thickness was selected for the main component, initially a NACA 6-digit airfoil (ref. [3]), in order to obtain a high curvature upper surface to better control laminar flow at low Reynolds number as well as provide room for fuel inside the wing and increase inertia of main spars. A similar design philosophy has been used by IAI for the UAV Heron (ref. [4]).

3.2 CFD Analysis

3.2.1 Variables and Objectives for Multipoint Optimisation

The objective of the final two-point optimal design is acceptable drag figures in cruise and take off conditions, achieving high lift coefficients in presence of flow regimes characterized by a Reynolds number that could fall below 1.0e06. The design objectives for the two-point optimization are resumed in the bullets below while design variables are shown in the next figure. The numerical optimization was carried on at C.I.R.A. on the basis of requirements issued by Galileo Avionica (Meteor at that time) coupling a genetic algorithm to a viscous-inviscid interaction method based on an Euler flow solver and an integral boundary layer routine; further details about the method can be found in ref. [5].

- DP #1 (LOITER-CRUISE): Minimum Drag at CL = 0.9 and Re = 1.3e06
- DP #2 (T/O-LAND): Minimum Drag at CL = 3.0 and Re = 1.0e06

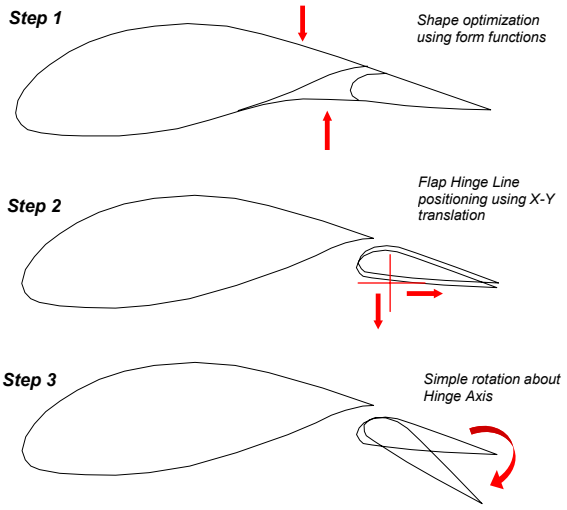

Figure 3: Multipoint optimization design variables

3.2.2 Airfoil Selection Process

The next figures shows a sample of the 75 airfoils generated by the optimization algorithm with their pressure distribution on each of the two design points.

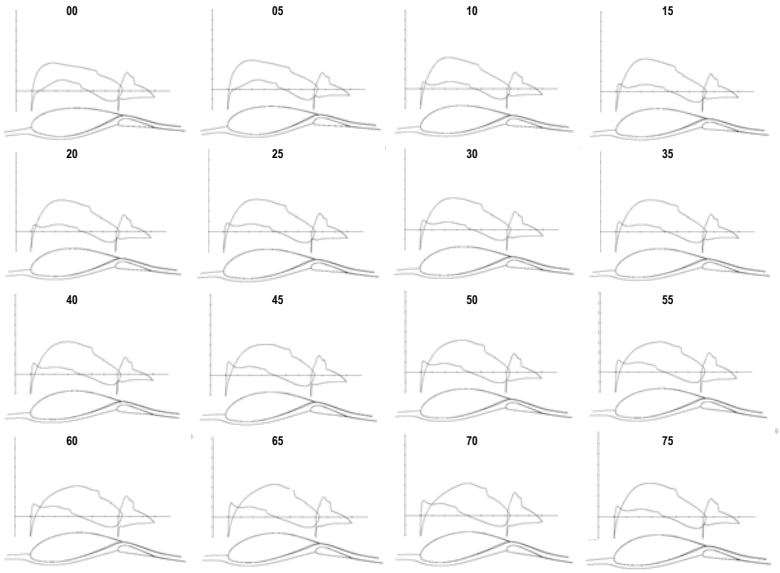

Figure 4: Generation of airfoils for DP #1 (CRUISE)

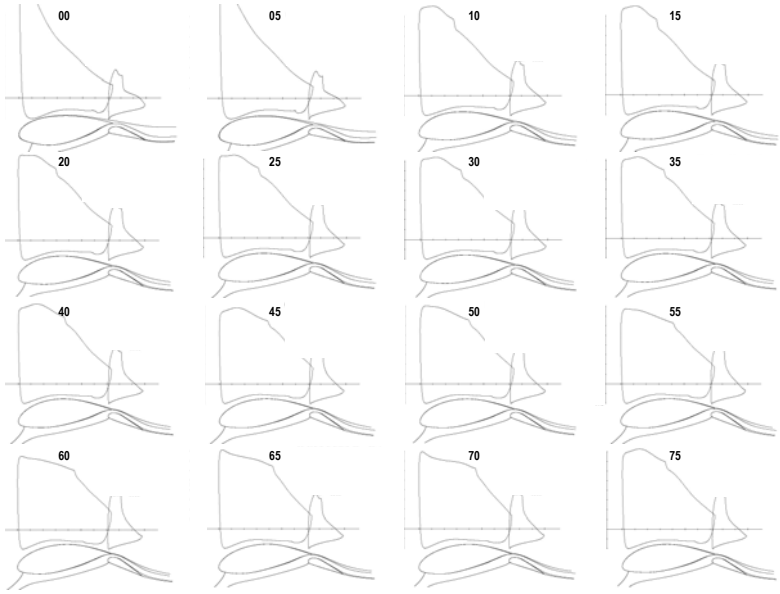

Figure 5: Generation of airfoils for DP #2 (T/O-LAND)

Airfoils in the upper left hand corner of figures 4 and 5 are optimized on design point 1, while airfoils on the lower right corner are optimized on design point 2.

The best compromise between the two design points is in the middle of each figure and in this area the final shape was selected as shown in next figure.

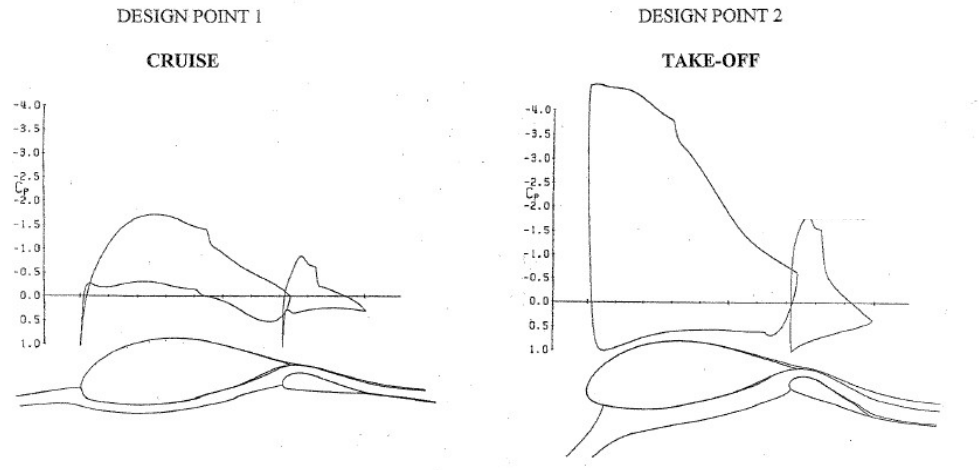

Figure 6: Selected airfoil with associated pressure distribution

The selected airfoil exhibits the following geometric and aerodynamic main features:

- Rounded blunt nose and high value of the Nose Shape Parameter (NSP) for the main element; these characteristics guarantee a smooth movement of the transition point on the upper surface with incidence and flap deflection, avoiding the rise of high suction peaks at the leading edge.
- Transition from laminar to turbulent flow is achieved on both design points through separation bubbles on the main element upper and lower surface and on the flap upper surface. The bubble

on the flap is of the "short type" (usually encountered in strong adverse gradients following a suction peak) while the two bubbles on the main element belong to the "long type" that shall be carefully examined for bursting (ref. [6]). These features are characteristic of the flow regime involved.

- The aerodynamic data for the two design points are as follow:
  - Angle of incidence is 0.962° in DP #1 and 12.783° in DP #2.
  - Flap deflection is +1.92° in the DP #1 and +15.76° in DP #2.
  - Airfoil L/D ratios are around 100 in both design points.

Further work was necessary after the selection of the best airfoil to achieve the final shape:

- Smoothing of the whole geometry to cancel small irregularities on the airfoil curvature introduced by the spline functions used for optimizing the overall shape.
- Introduction of trailing edge finite thickness compatible with construction of the wing using composite materials.

3.2.3 Laminar Transition Bubbles Stability Analysis

The three laminar transition bubbles have been studied with particular emphasis on:

- Effect of free stream turbulence
- Stability with decreasing Reynolds number ("Bubble bursting")

The effect of free stream turbulence has been verified by checking that no major changes in the boundary layer, except an overall drag increment, exist when the free stream turbulence is raised until a fully turbulent flow develops; In effect blunt nose airfoils can be prone to an "adverse effect" which means a decrease of maximum lift when Reynolds number and/or turbulence level is increased from the design point (ref. [7]).

The numerical analysis showed that the selected airfoil performs well over the whole range of situations tested, being able to maintain its lift characteristics from very low Reynolds number to the values expected in flight without showing any sign of adverse effect.

A sample of the CFD simulations performed is shown in the next figure.

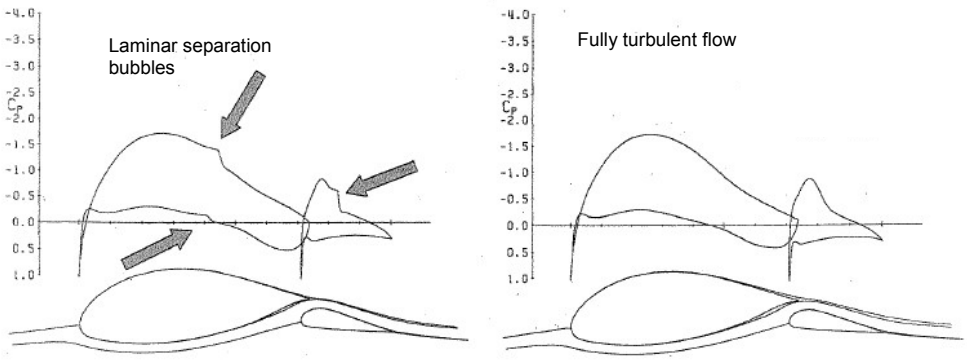

Figure 7: Effect of free stream turbulence on laminar transition bubbles

The effect of free-stream turbulence has been studied both by forcing a fully turbulent boundary layer in the viscous-inviscid interaction flow solver at C.I.R.A. and by analyzing the effect of increasing free-

stream turbulence using a 2-D multi component panel method coupled to an integral boundary layer calculation method developed by the author at Galileo Avionica; the boundary layer formulation is similar to that described in the computer program of Prof. R. Eppler (ref. [17]).

Both methods showed that a forward shift in the transition point due to an increased turbulence level simply increases the overall airfoil drag without major influences on maximum lift figures.

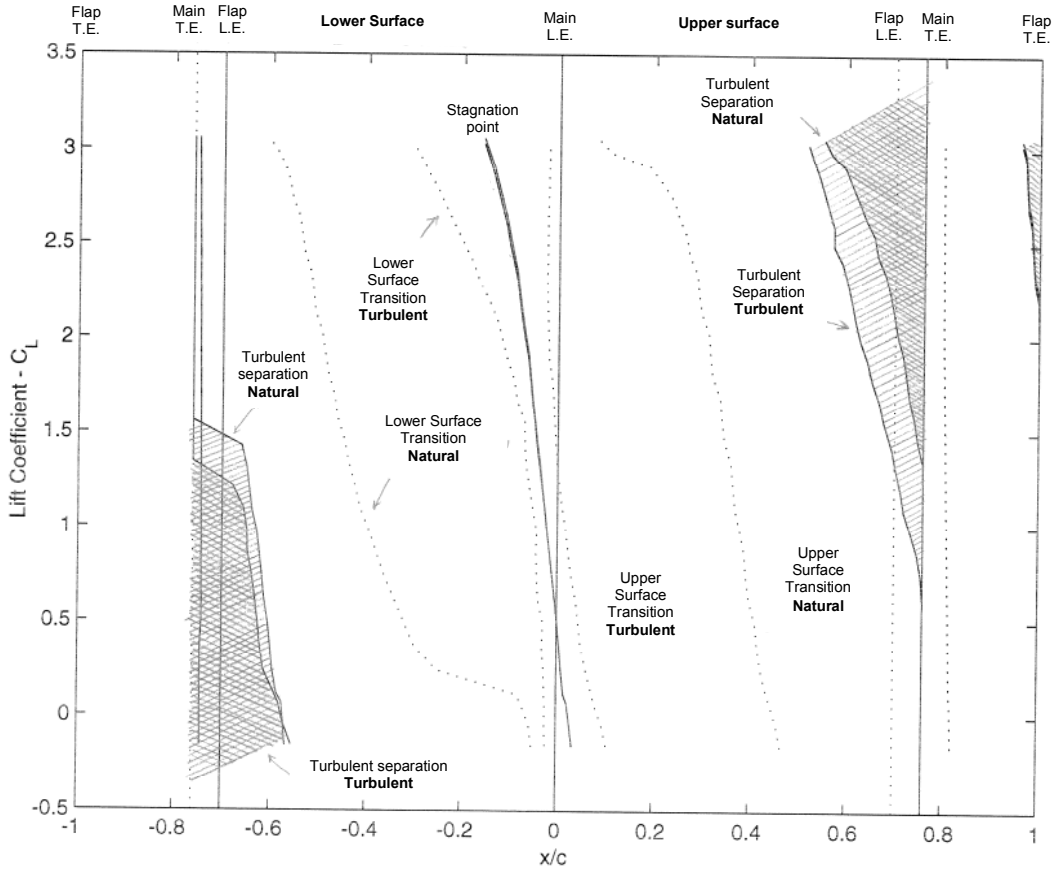

Figure 8: G.A. B.L. code: effect of free stream turbulence– (no viscous-inviscid interaction)

The figure above shows an analysis of the transition and separation point shift due to turbulence using the Galileo Avionica integral boundary layer calculation method on the 2-D inviscid pressure distribution.

Due to the absence of any interaction large maximum lift coefficients are encountered since stall phenomena are not correctly simulated except for a large trailing edge turbulent separation that increases smoothly with incidence (ref. [8]). No divergence of the separation point with incidence is observed, confirming the good behavior with incidence and turbulence intensity level. The turbulence intensity is taken into account using the method of ref. [2].

The large turbulent separation on the main element lower surface was not present in the C.I.R.A. calculations using the interactive flow solver: the boundary layer separates in the pressure "valley" just before the flap leading edge due to the lack of interaction between the boundary layer and the inviscid pressure distribution (ref. [18]), which doesn't account for the large displacement thickness actually "smoothing out" the adverse pressure gradient and consequently avoiding separation prior to the suction peak induced by the flap. This separation effect was not considered and subsequent wind tunnel tests proved this assumption to be correct.

The behaviour of laminar transition bubbles is very important at low Reynolds numbers and their stability has been studied by many authors, some pioneers being Crabtree (ref. [9]), Young & Horton (ref. [10]), and Gaster (ref. [11]) who worked to find out simplified prevision formulae to predict if a bubble would burst or not depending on the characteristics of the boundary layer at separation.

In all the CFD simulations performed none of the three separation bubbles showed any tendency to burst, anyway an analysis was performed in order to check their robustness with respect to complete, massive flow separation using the classic method (on the assumption that "simpler is always the best") of Gaster, who related the Reynolds number calculated on the displacement thickness at separation $Re_{\theta S}$ to the pressure parameter P described by the following formula for bubbles about to burst:

$$P = \frac{\theta_S^{\,2}}{\nu}\frac{\Delta U}{\Delta X}$$

where $\Delta U / \Delta X$ is the average pressure recovery over the bubble length, θ_S is the displacement thickness at separation and ν is the kinematic viscosity coefficient.

Some results of the stability analysis are shown in the next figure, where it can be seen that none of the bubbles trajectories intersect the bursting line down to a Reynolds number of 500.000.

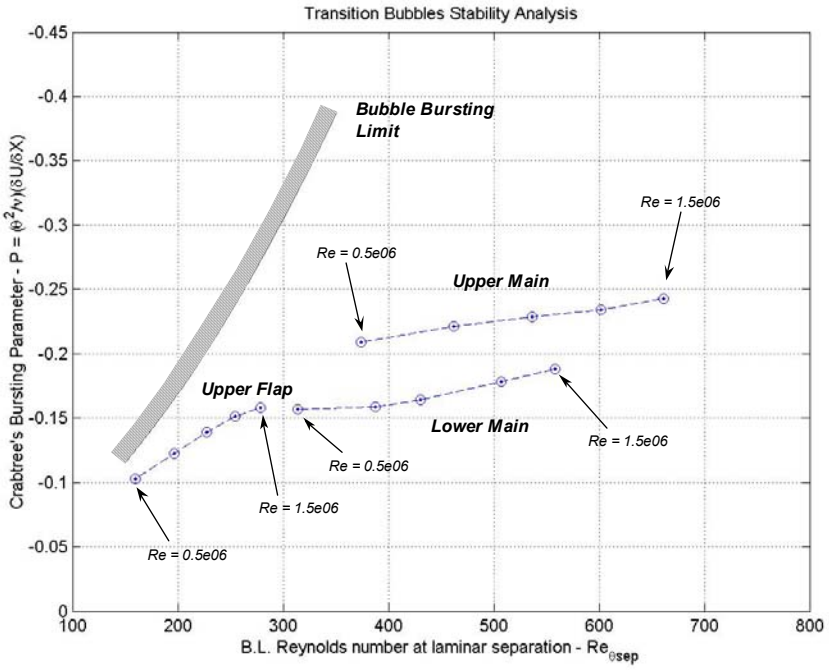

Figure 9: Laminar bubble stability analysis

3.2.4 2-D Ice Accretion Analysis

Additional in-flight icing analysis through computer simulation were performed by Alenia Aeronautica in the frame of the contract for wind tunnel tests of the 2-D airfoil, in order to provide information about residual performance in icing conditions; the in-flight icing conditions described below, selected according to ACJ 25.1419, have been used for calculation purposes:

- 3 minutes flying in Intermittent Maximum Icing Conditions (IMIC);
- 10 minutes flying in Continuous Maximum Icing Conditions (CMIC);
- Droplet diameter (MVD): 20 μm;
- CMIC Liquid Water Content (LWC): 0.62;
- IMIC Liquid Water Content (LWC): 2.55;
- Outside Air Temperature (OAT) at different altitudes variable between –5 °C and –18 °C.

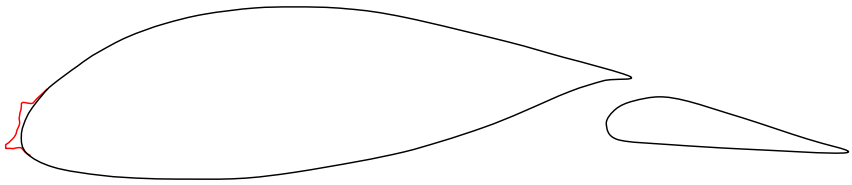

α = -1.16, TAS = 50 m/s, T = -9 °C, LWC = 0.62 g/m^3, MVD = 20 μm, Time = 600 sec

Figure 10: Ice accretion calculation - worst ice shape and associated conditions

The ice shape shown in the previous figure was selected as the most dangerous and consequently a resin model was realized in order to test the airfoil performance in the wind tunnel, as discussed in paragraph 3.3.1.

3.2.5 3-D CFD Analysis

Complete aircraft aerodynamics has been studied using the well-known panel code VSAERO.

For the purpose of wing analysis only the wing-body configuration is of interest; the next figure shows a result of the VSAERO output for a representative flight condition.

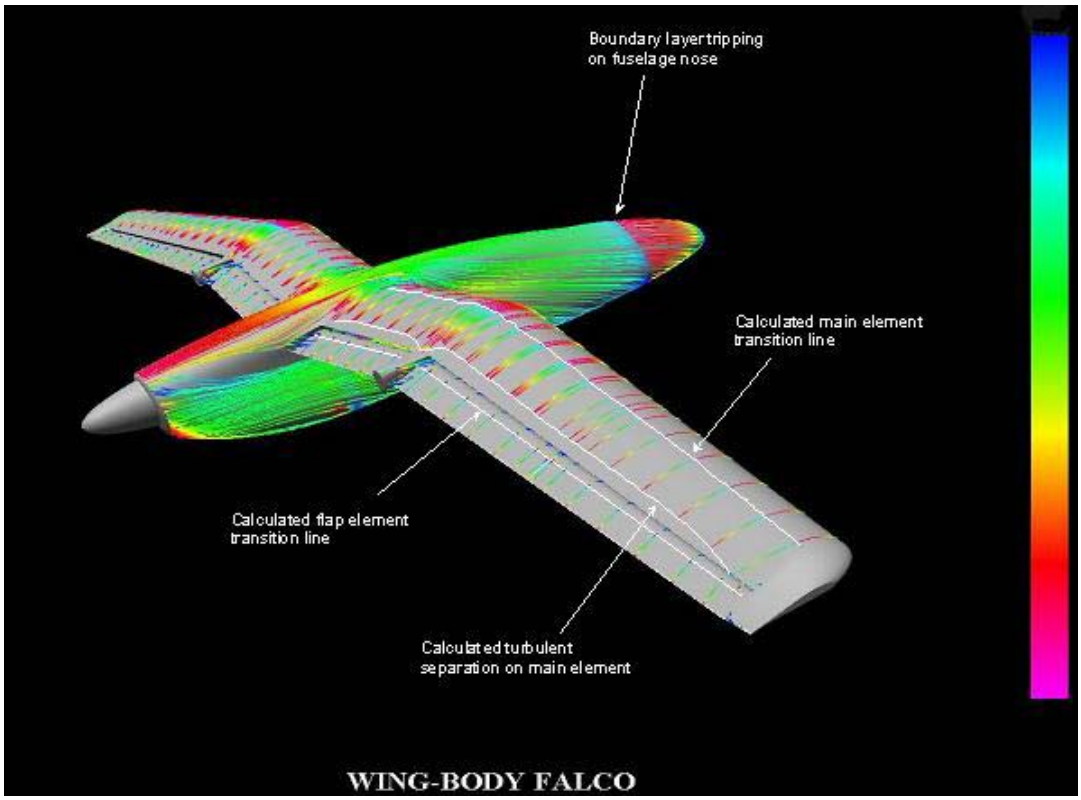

Figure 11: VSAERO streamlines and associated skin friction coefficient

The VSAERO boundary layer routine uses an integral calculation method running downstream from each stagnation point along surface streamlines calculated using the potential flow solution; transition is assumed to occur if early laminar separation is encountered, consequently the transition lines shown in the previous figure actually represent the separation position. As a consequence of this approach a large turbulent separation is predicted on the main element upper surface close to the trailing edge, as found with G.A. 2-D code (see para. 3.2.3). This separation is not expected under normal flow conditions.

To obtain "close to real" performance data for the complete aircraft potential flow lift and drag distribution over the wing span where corrected using 2-D data by means of a "strip theory" approach.

3.3 Wind Tunnel Testing

Wind tunnel tests have been executed on the full scale 2-D airfoil and on a model of the complete aircraft in the Alenia Low Speed Wind Tunnel (ALSWT) in Turin, Italy.

3.3.1 2-D Wind Tunnel Testing

Two dimensional wind tunnel tests have been performed on a full-scale model of a wing section with a chord of 650 mm and a span of 600 mm.

To achieve two dimensional flow despite of the low aspect ratio of the wing section model and the strong adverse pressure gradients that develop in the flow field, especially at the higher angles of incidence and flap deflection, a boundary layer suction system on the tunnel walls was set up by the Alenia wind tunnel engineers. The system operated by aspiring the wall boundary layer at some fixed chordwise stations due to high pressure "ejectors" located in a channel just behind the wall.

The aluminum-machined model was instrumented with an internal balance for a quick reading of forces and pitching moment and with over 100 pressure taps able to provide the detailed pressure distribution over the main and flap elements of the wing section.

A wake rake for drag measurements was installed about 1 chord length downstream the wing section.

Pressure measurements in the two design points showed a fairly good agreement with the calculations, as shown in the next figure.

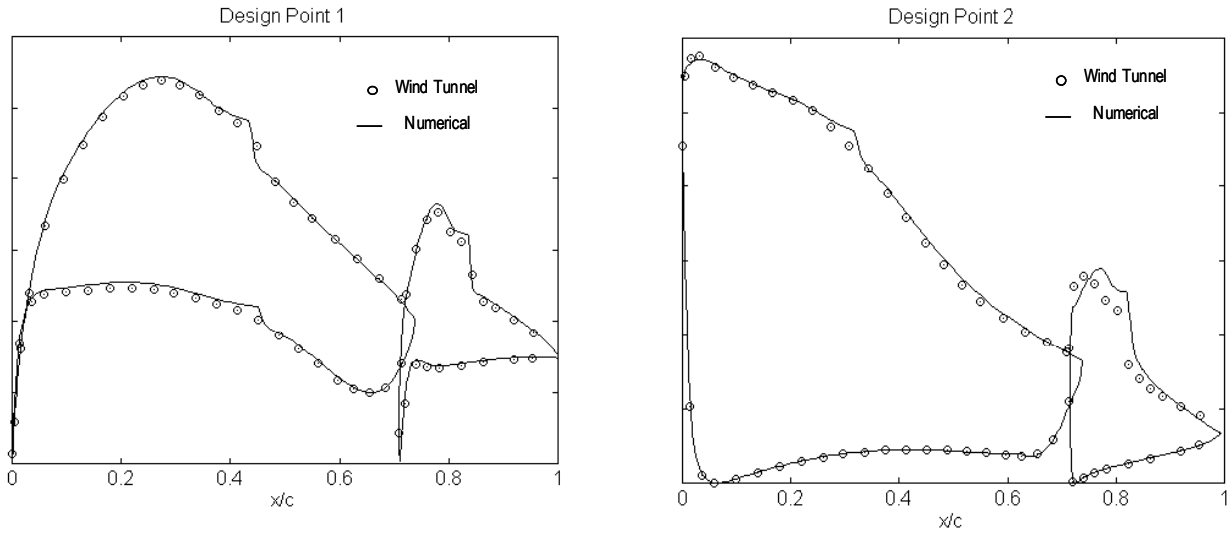

Figure 12: Experimental pressure distribution in the two design points

The wind tunnel main session of tests confirmed the results of the CFD analysis even if a slight adverse effect (10% loss of lift) was observed in the performance of the wing section: maximum lift coefficient actually decreasing with free air stream speed.

The adverse effect was attributed to the air pressure in the boundary layer suction system, that was calibrated at 4 atm during preliminary runs executed at low speed (16.5 m/s) and was not probably capable to deal with the higher airspeeds tested (up to 45 m/s).

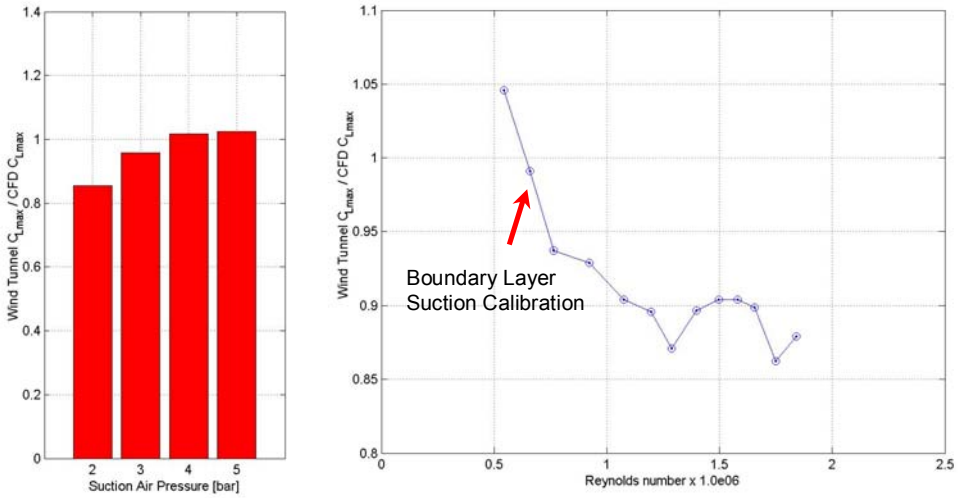

Figure 13: Effect of boundary layer suction on wing section maximum lift

Another difference that was observed during the main session of tests was some uncertainty in bubble behavior, whose presence was rarely observed on the main element even at the lowest Reynolds numbers.

To investigate this phenomenon, a turbulence survey was performed using an hot wire anemometer from the University Politecnico of Turin; the measurements taken inside the two-dimensional channel, close to the airfoil leading edge, showed a free stream turbulence level about 0.94% (Tu = 0.0094) that, according to Pope (ref. [20]) is equivalent to a 75.2% increase in free stream Reynolds number as evaluated with the classical method of turbulence spheres.

Free stream Reynolds number effect on laminar separation bubbles has been studied by several authors like Van Ingen (ref. [12] and [13]) and Selig & Maughmer (ref. [14]) and its prevision is a quite delicate matter. A clear explanation of what happened during the tests is still unclear, also because the distribution of pressure tappings on the airfoil was too coarse to adequately capture the bubble shape; what can be argued is that the higher turbulence level probably caused some changes in the mechanism of transition not necessarily favorable to improve measured wing section performance, especially in terms of overall drag.

Many researchers have designed airfoils for low Reynolds number, attempting to minimise the negative effects of separation bubbles as M. Selig (ref. [14]), Horstmann & Quast (who have also studied the effect of pneumatic turbulators, ref. [15]), Wortmann (ref. [16]) and the above mentioned Prof. R. Eppler (ref. [17] and [19]) who can be probably considered the “pioneer” of low speed airfoils.

Drag figures were calculated by measuring the momentum loss using the wake-rake installed on the centreline of the 2-D channel. Accurate measurements were possible only at low angle of incidence and higher speeds due to the low sensitivity of the pressure transducers connected to the wake rake; these measurements showed a quite high drag if compared to the CFD values: actual figures being about 20% higher than the expected. Such an effect is probably related with the high free stream turbulence level discussed above since no laminar bubbles where observed elsewhere than on the flap suction side during minimum drag tests.

The next figure shows on the left hand side the wing section (with a simulated ice shape on the leading edge) installed in the two-dimensional chamber and the wake rake in the background; on the right hand side a sample of the velocity profiles measured.

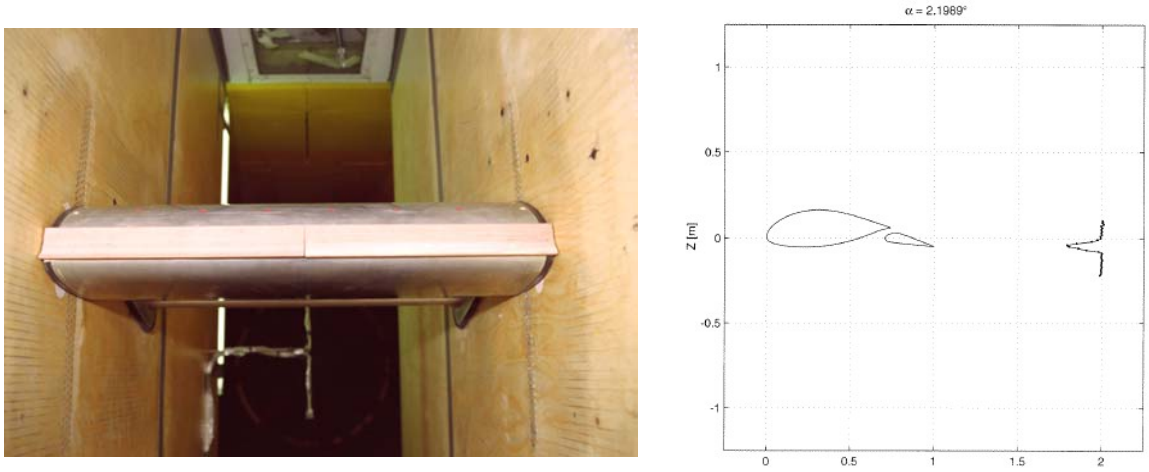

Figure 14: Wing section model installed in the tunnel and sample wake survey output

The degradation in aerodynamic performance due to icing was investigated using the ice shape model realized according to calculations performed by Alenia Aeronautica as described in para. 3.2.4.

Tests were executed at high Reynolds number and the results showed maximum lift decreasing about 30% almost independently of flap deflection; taking into account the 10% loss for the clean airfoil due to boundary layer suction discussed earlier the total loss of lift is expected to be about 40% following 10 minutes flying at 1000 m in continuous icing conditions.

These results are in accordance with the theory of Brumby (ref. [21]) that indicates a loss of lift coefficient between 30% and 40% and with experimental results attained on a similar philosophy airfoil section (ref. [22]).

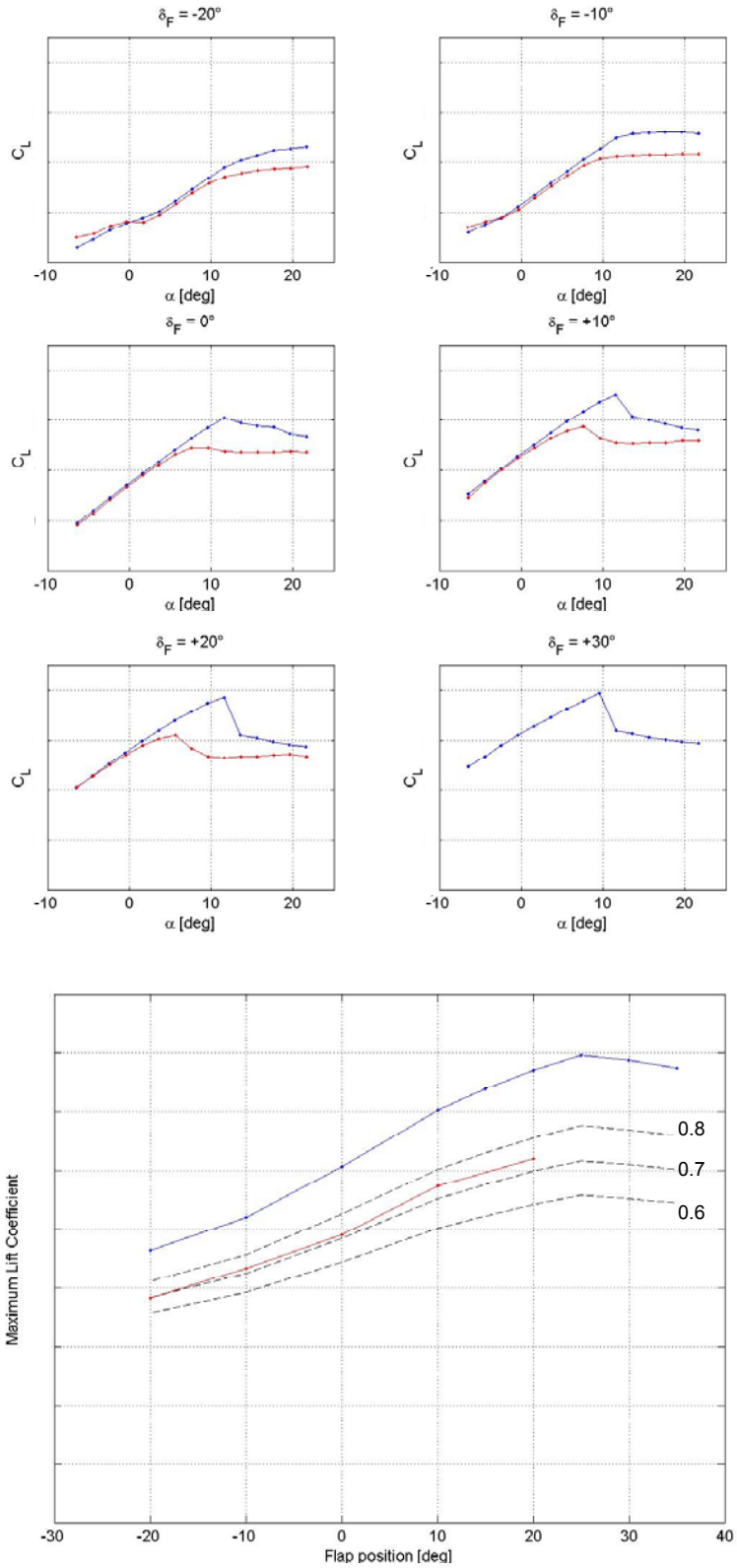

Figure 15: Degradation of lift characteristics due to icing (High Reynolds number configuration)

3.3.2 3-D Wind Tunnel Testing

Three dimensional wind tunnel tests of the UAV were executed using a 1:4.5 scale model of the complete aircraft configuration; the model allowed a build up of the configuration starting from body-alone, body-wing, body-wing-tail etc. up to include payloads, antennas and protuberances.

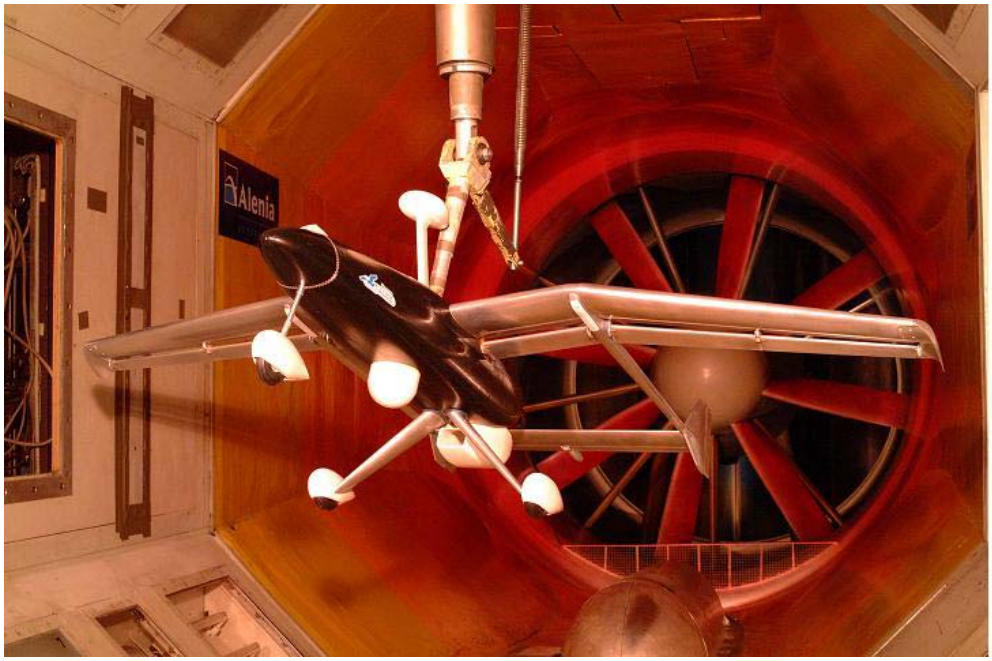

Figure 16: FALCO UAV 1:4.5 complete configuration model in the ALSWT.

Prior to the execution of 6-axes internal balance measurements a preliminary survey with the technique of the colored oils were executed on the wing-body assembly in order to assess the correct flow behavior at low Reynolds numbers and high angles of incidence. The model nominal Reynolds number was about 500.000, even if free-stream turbulence probably still played a role in increasing the effective Reynolds number (ref. [23]), but despite of this no boundary layer tripping was required on the wing surfaces to reach the stall angle of incidence.

The oil flow visualizations were in fair agreement with the previsions of the CFD analysis work and previous 2-D wind tunnel tests, confirming almost all of the observed flow features: laminar bubbles were stable even at low Reynolds numbers, no regions of reversed flow were visible on the wing upper surface until a smooth stall starts at 2/3 of the wing span exactly as predicted by the strip-theory analysis.

The next figure shows an example of the oil flow visualization in the same condition of figure 11.

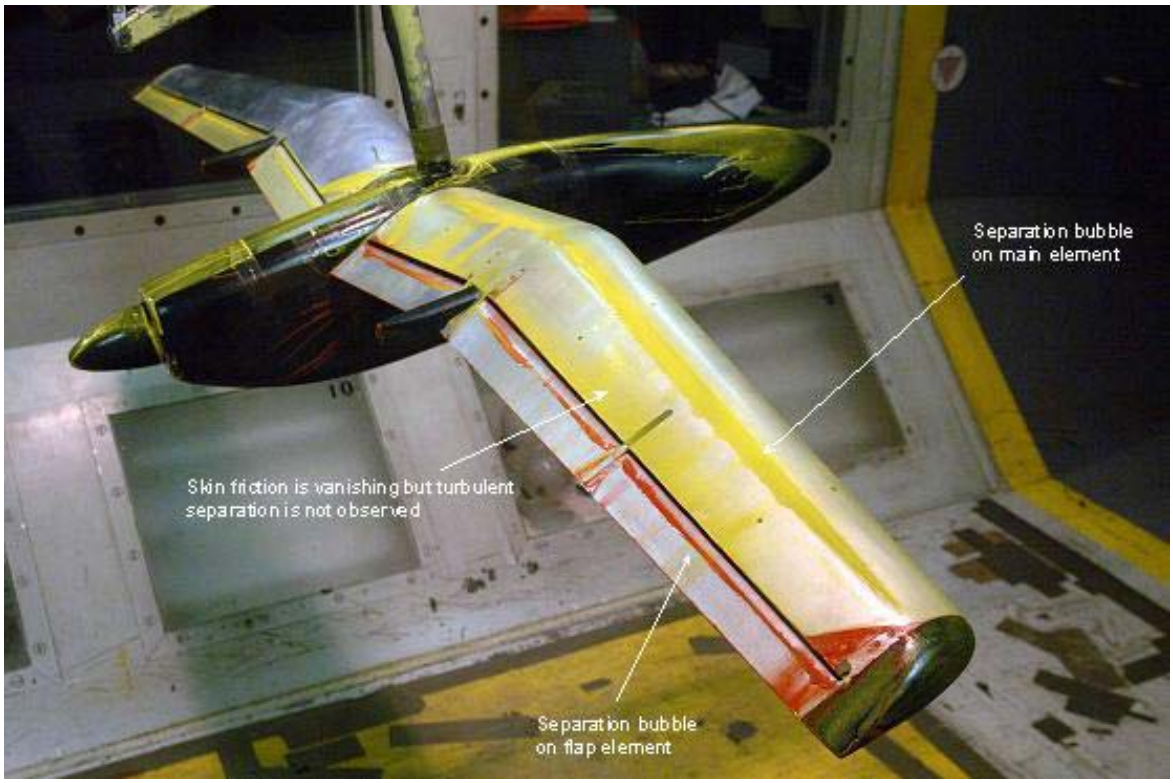

Figure 17: Oil flow visualization

The 6-axes balance measurements confirmed the overall maximum lift coefficient figures of the design, but at this stage it was still not possible to definitely state that the inverse Reynolds effect observed during 2-D tests was caused by insufficient boundary layer suction on the channel walls; anyway the 3-D tests cleared out any doubt about the possibility of the boundary layer suction "helping" the airfoil in getting its maximum lift as the maximum lift coefficient and stall features where very close to the theoretical previsions.

Elevator effectiveness proved to be satisfactory up to and beyond stall angle of incidence, while overall efficiency and ceiling parameter (including landing gear, payload and "protuberances") were fully satisfying with numerical values very close to the expected ones.

The availability of comparative wind tunnel tests carried on at ALSWT as part of a thesis work (ref. [24]) on a UAV model of the same size allowed to verify overall design effectiveness. The wing of the UAV used for comparison was designed with a conventional NACA six digits airfoils and a conventional, trapezoidal planform with AR = 8.

The maximum L/D ratio of the FALCO UAV is about 20% higher than the value achieved by the comparative UAV of different design; moreover, the maximum climb parameter is about 50% higher in the same conditions, confirming the effectiveness of the design philosophy adopted.

3.4 Flight Trials

A FALCO UAV prototype obtained in June 2005 a "Permit to Fly" from the Italian Civilian Authority ENAC in order to investigate some basic flight characteristics as a preliminary research and development activity for the final certification of the system; the air vehicle got the temporary tail-number I-RAIE.

A systematic investigation of performance and flying qualities of the aircraft was carried on by extensive flight testing on the firing range of PISQ in Sardinia, providing an excellent safe place for flying since it is not active for military exercises during the summer season.

Flight-tests mainly involved stall, climb and handling characteristics according to ref. [25] and [26].

As part of this activity the aircraft was stalled almost in every foreseeable condition of flap position, power setting and autopilot mode either in “fully manual” mode (A/P Off) or “Assisted” mode (A/P On); accelerated, yawed and “deep stalls” were also executed to complete the frame.

Figure 18: Falco UAV prototype air vehicle I-RAIE

The aircraft proved to have satisfying stall characteristics (very soft stall) in all the conditions tested. Airfoil cleanliness was not assessed with specific tests but the usual dirt encountered in normal flying activity from semi-prepared airstrips in summer season accumulated on the leading edge (insects, dust etc.) was present, moreover, the test aircraft was painted with camouflage scheme using a mat paint that provided a rough surface if compared, as example, to gel-coated wings of sailplanes.

None of these features appeared to influence wing performance; subsequent flight activities, even if not directly devoted to further investigate stall characteristics, were executed with many different atmospheric conditions, including rain, and did not evidence any abnormal aircraft behavior at low speed.

Level flight stalls in manual mode (A/P off) were executed according to ref. [26], the aircraft was trimmed at 1.1 to 1.2 times the stall speed then power was cut progressively attempting to maintain level flight until stall.

Next figure shows an example of the aircraft telemetry during a stall maneuver executed in “manual” mode, with flaps positioned in the nominal “LOITER” position (deflection zero degrees).

The stall condition was hold for about 25 seconds in order to evaluate aircraft controllability in a post-stall attitude and despite of this the aircraft remained stable and controllable, loosing just 150 m of altitude during the maneuver until level flight was achieved again maintaining the aircraft in a low speed condition using power to verify minimum flying speed.

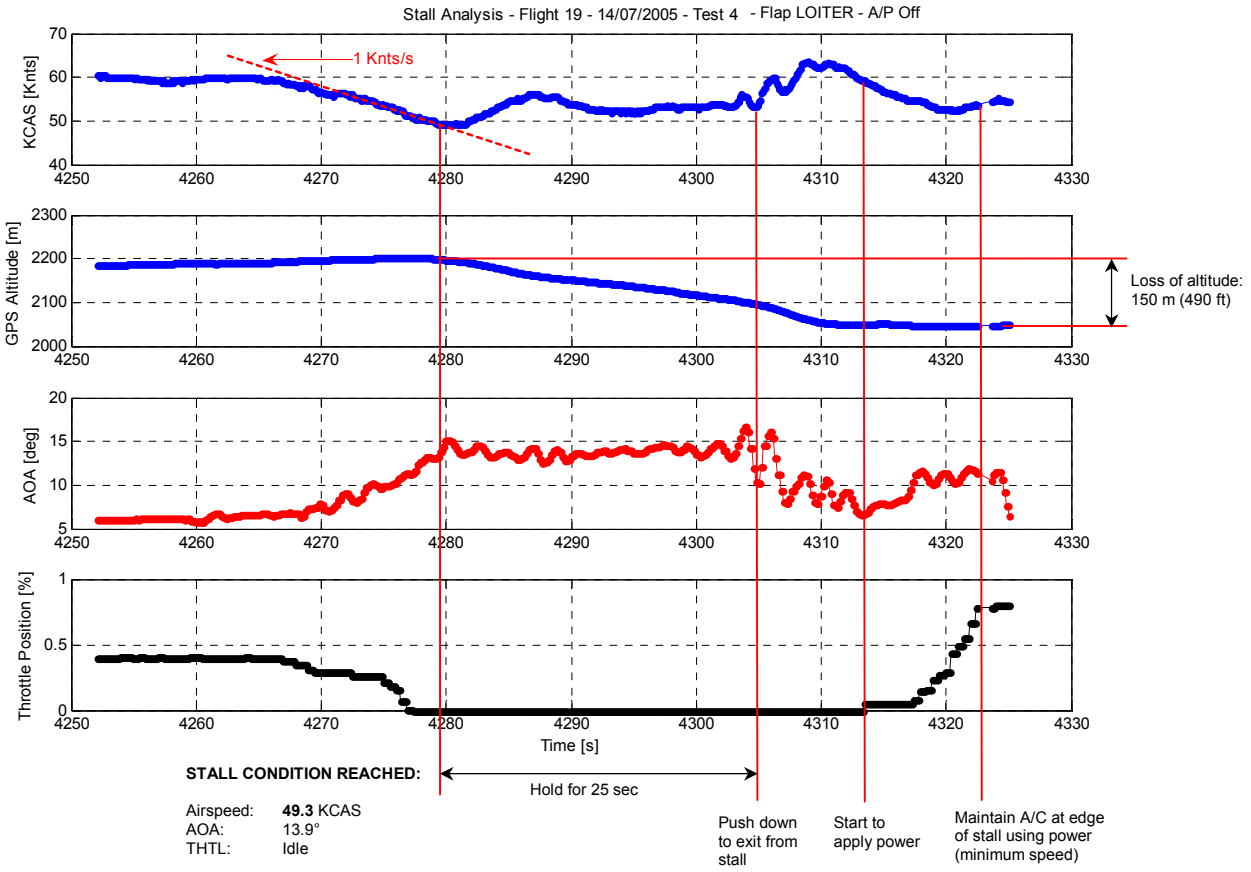

Figure 19: Example of telemetry during a stall maneuver

For what concerns about flight characteristics other than stall speed, cruise and climb performance were in good agreement with calculations from the aerodynamic point of view, the major concern being the effective evaluation of propeller performance due to the unknown interference effect of the fuselage (the propeller is in a pusher configuration and the prototype air vehicle mounted a direct drive propeller with a relatively smaller diameter if compared to production aircraft).

Next table is a resume of some of the stall condition tested: switching A/P On and OFF changes the amount of elevator used to hold the stall condition as a result that the autopilot simply uses all the available deflection trying to keep the pitch attitude constant while the pilot is allowed to utilize just a fixed, partial amount in order to avoid excessive g-loads on the structure; this in fact doesn't limit the overall maximum lift coefficient achieved since the aircraft is deeply stalled in both A/P modes, confirming that the elevator's authority is sufficient to reach the peak value of lift coefficient in the configuration tested.

Table 2: Some stall test results using prototype I-RAIE

Flap Position	*A/P Mode*	*C.o.G. Position*	CL_{max} / CL_{maxDES}	*Elevator [deg]*
CRUISE	OFF	Aft	+1.7%	78% UP
CRUISE	OFF	Aft	+3.3%	78% UP
CRUISE	OFF	Aft	+1.1%	78% UP
LOITER	OFF	Aft	-2.0%	69% UP
LAND	OFF	Aft	-7.3%	37% UP
LOITER	ON	Aft	-1.7%	Full UP
LAND	ON	Aft	-7.3%	Full UP

The maximum lift coefficient for the flight trials and the 3-D wind tunnel tests is evaluated on the basis of the "exposed flapped planform area" that is roughly 90% of the total projected wing area as it is usually defined (hypothesis of fuselage carry-over): this inherently gives figures of C_L that can be directly compared to the 2-D design and wind tunnel values as shown in the next figure.

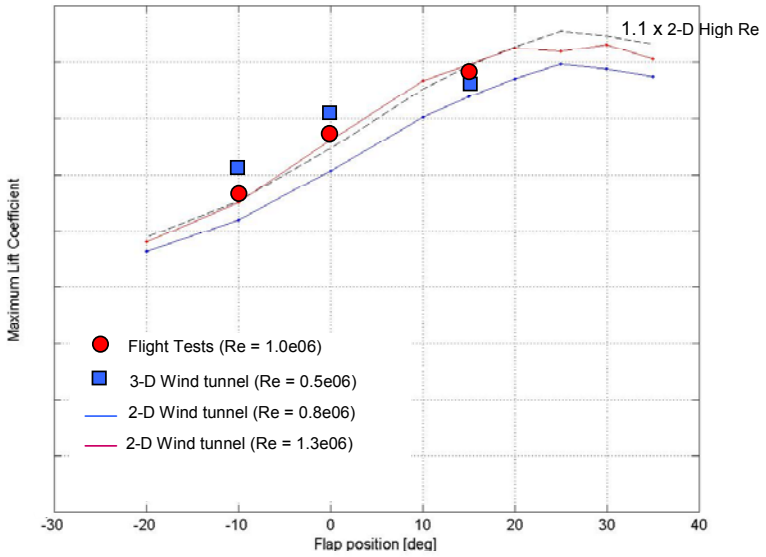

Figure 20: Wing section maximum lift coefficient vs flap deflection from various different tests

4.0 FUTURE WORK

To further improve the performance of the wing design, it would be desirable to investigate the possibility to modify the flap movement from a simple rotation to a fowler, adding a degree of freedom to the optimization problem by allowing flap hinge position changing from one design point to another.

This feature would allow optimizing the landing performance by increasing the drag of the wing while maintaining its excellent lift characteristics; a considerable drag increment is desirable in order to increase the ramp angle during descent, shortening the flight distance when landing over a usual 50 ft obstacle.

About testing, a comprehensive in-flight survey of different leading edge disturbances (tripped transition, simulated ice-shapes etc.) would be desirable to definitely assess airfoil robustness with respect to operational environment.

5.0 CONCLUSIONS

A complete airfoil design and test activity has been presented from the preliminary stage of setting up suitable requirements to the final flight testing of a complete aircraft going through intermediate CFD analysis and wind tunnel tests. Many problems encountered during the development and testing have been studied and properly addressed through systematic investigation and switching of analysis methods, ranging from very simple correlation formulae to state-of-the-art CFD software.

Results from the many different analysis and test activities show a good correlation, keeping in mind the different flow conditions that have strong influences on the flow behavior at such low Reynolds numbers.

Acknowledgments

Many people from companies other than Galileo Avionica have worked to the activities described in this paper under contracts or cooperation agreements.

The author wish to aknowledge D. Quagliarella, G. Mingione and L. Paparone from C.I.R.A. who carried on the optimisation work and performed the initial CFD analysis; M. Di Muzio from Alenia Aeronautica who performed the ice accretion analysis; A. Gatti, P. Gilli, P. Miola and all the personnel of ALSWT who were absolutely professional and really precious during all of the wind tunnel tests; Prof. Iuso and Spazzini of the University Politecnico of Turin who operated the hot wire anemometer for the free-stream turbulence survey during 2-D wind tunnel tests.

Last but not least, it is a must to acknowledge all the colleagues from Galileo Avionica, whose names is practically impossible to file in this page, who have worked hard on the design and test of the UAV Falco.

REFERENCES

[1] *Impact Energy Method For Establishing The Design Standards For UAV Systems,* Appendix to *JAA/Eurocontrol UAV Task-Force Final Report*, Enclosure 3, May 2004.

[2] Eppler R., *Turbulent Airfoils for General Aviation,* Journal of Aircraft, Vol. 15, No. 2, February 1978.

[3] Abbott I., Von Doenhoff A.E., *Theory of Wing Sections*, Dover Pub., 1959.

[4] Vitali J., Tsach S., Avni H., Gali S., Weissberg V., *Development Approach of the Heron Medium Altitude Long Endurance UAV*, ICAS Conference Proceedings, 1996.

[5] A. Vicini, D. Quagliarella, *Inverse and Direct Airfoil Design Using a Multiobjective Genetic Algorithm,* AIAA Journal, Vol. 35, No. 9, Sep. 1997.

[6] Steinheuer J., *Boundary Layer Calculation Methods and Application to Aerodynamic Problems*, AGARD LS-67.

[7] Yoshida K., Ogoshi H., *Study of Reynolds Number Effect on Clmax of 2-Dimensional Airfoils*, ICAS Conference Proceedings, 1996.

[8] Katz J., Plotkin A., *Low-Speed Aerodynamics*, McGraw-Hill, 1991.

[9] Crabtree L.F., *The Formation of Regions of Separated Flow on Wing Surfaces,* R and M 3122, 1959.

[10] Young A.D., Horton H.P., *Some Results of Investigations of Separation Bubbles,* AGARD CP-4, Separated Flows, 1966, Part 2.

[11] Gaster M., *The Structure and Behaviour of Laminar Separation Bubbles,* AGARD CP-4, Separated Flows, 1966, Part 2.

[12] Ingen J.L. van, *On the Calculation of Laminar Separation Bubbles in Two-Dimensional Incompressible Flows.*

[13] Ingen J.L. van, *Transition, Pressure Gradient, suction, Separation and Stability Theory*, AGARD CP-224, May 1977.

[14] Dini P., Selig M., Maughmer D., *Simplified Stability Transition Prediction Method for Separated Boundary Layers,* AIAA Journal, Vol. 30, No. 8, August 1992.

[15] Horstmann K.H., Quast A., Boermans, *Pneumatic Turbulators – a Device for Drag Reduction at Reynolds Numbers below* $5x10^6$*,* AGARD CP 365.

[16] Wortmann F.X., *Ueber den Ablösewinkel laminarer Ablöseblasen, DLR-FB-74-62, 1974.*

[17] Eppler. R., Somers D.M., *A Computer Program for the Design and Analysis of Low-Speed Airfoils,* NASA TM-80210, 1980.

[18] Drela M., Giles M.B., *Viscous-Inviscid Analysis of Transonic and Low Reynolds Number Airfoils, AIAA Journal*, Vol. 25, No. 10, 1987.

[19] Eppler R., *Airfoil Design and Data,* Springer Verlag, 1990.

[20] Pope A., Harper J.J., *Low Speed Wind Tunnel Testing,* John Wiley & Sons, New York, 1966.

[21] Lee S., Kim H.S., Bragg M.B., *Investigation of Factors that Influence Iced-Airfoil Aerodynamics*, 38th Aerospace Sciences Meeting & Exhibit, USA, 2000.

[22] Shepshelovich M., *UAV Wing Design - A New Challenge*, Journal of Aerospace Sciences and Technologies, Aeronautical society of India, Vol 57, Numb 1, 2005.

[23] Otto H., *Systematical Investigations of the Influence of Wind Tunnel Turbulence on the Results of Model Force-Measurements*, AGARD CP-174.

[24] Golzio A.L., *Studio del comportamento aeromeccanico di un velivolo UAV con prove in galleria del vento*, Thesis Work (in italian), Politecnico di Torino, March 2001.

[25] MIL-F-8785C, *Flying qualities of piloted airplanes*.

[26] AC 23-8A, *Flight Test Guide for Certification of Part 23 Airplanes*, FAA, 09/1989.